Characterization of Flicker Noise in GaAs MESFET's for Oscillator Applications

Paul A. Dallas, *Associate Member, IEEE*, and Jeremy K. A. Everard, *Member, IEEE*

***Abstract*—GaAs MESFET oscillators commonly exhibit increased close-to-carrier noise, which is often attributed to upconversion of flicker noise from the MESFET. To establish and quantify this effect, this paper presents an experimental system that allows the simultaneous measurement of the flicker noise on the gate and drain terminals of a GaAs MESFET, and of the noise imposed on an RF carrier when amplified by the MESFET. The cross correlations between these parameters can thus be determined; an analytical method is shown for extracting the levels of the effective sources of flicker noise from the results, and the manner in which these affect the RF carrier. In the tests performed, it was often found that the close-to-carrier noise was related directly to the low-frequency flicker noise.**

***Index Terms*—Flicker noise, MESFET, , oscillator, phase noise.**

I. Introduction

GaAs MESFET's are used extensively in microwave oscillators. They provide relatively high output powers with high efficiency, are reliable in operation, and have convenient power-supply requirements. However, although GaAs MESFET's generate little noise at high frequencies, oscillators using them generally exhibit large amounts of sideband noise close to the carrier.

GaAs MESFET's generate high levels of low-frequency (LF) flicker noise, with an approximate f^{-n} power spectrum, where f is the frequency and $n \approx 1$. The high level of noise close to the carrier in GaAs MESFET oscillators is commonly attributed to this LF flicker noise, which is believed to be modulated onto the carrier through the intrinsically nonlinear behavior of the MESFET ([1]–[5], but also see alternative explanations in [6] and [7]). The flicker noise is said to be generated by carrier-generation–recombination (g–r) centers (traps) in the gate and substrate depletion regions of the FET [8]–[12], g–r centers on the surface of the FET [10], [13], and by lattice scattering [14], [15] and g–r centers [16] in the conducting channel. Hashiguchi *et al.* ([17]) have developed a GaAs MESFET LF equivalent circuit to represent such flicker noise sources. An extended version of this circuit is shown in Fig. 1.

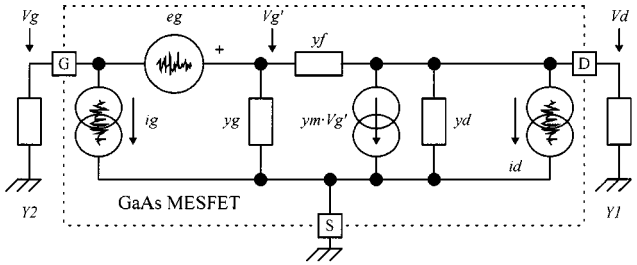

Fig. 1. General GaAs MESFET model showing the effective flicker noise sources and nonlinear (trans)admittances. $Y1$ and $Y2$ represent the inputs of the noise measuring system.

In order to reduce the close-to-carrier oscillator noise, attempts have been made in the past to reduce both the flicker noise itself and its conversion to noise sidebands. Many of the methods shown in literature, however, have been found to be less effective than expected [18]–[21]. One of the reasons for this may be the inaccurate representation of the flicker noise sources in the theoretical analyses upon which these methods are based. In order to calculate the levels of flicker noise reaching the nonlinear elements of a GaAs MESFET, a quantitative knowledge of the magnitudes and cross-correlation coefficients of the flicker noise sources is required. As, to our knowledge, there has not hitherto been a comprehensive method for determining these, it has been common practice to omit some of the noise sources shown in Fig. 1 or to make assumptions about their levels and cross correlations.

This paper presents a measurement-oriented technique for determining the levels of these equivalent flicker noise sources, the cross correlation between the gate sources eg and ig, and the effect the flicker noise sources have on a high-frequency carrier when this is amplified by the MESFET. This technique is based on the analytical extrapolation of the equivalent flicker noise source parameters from measurements of the LF and the modulation flicker noises generated by the GaAs MESFET under test.

II. The GaAs MESFET Noise Measuring System

The noise measuring system is an extended version of the phase bridge arrangement presented by Riddle and Trew [22] and Sann [23]. An early version of this system, capable of measuring the cross correlation between the LF drain and modulation noises of a GaAs MESFET, was demonstrated by the authors in [24]; more recently, Martinez *et al.* [21] presented a system for measurements on a pseudomorphic high electron-mobility transistor (pHEMT). The new system described here adds the capability of measuring the LF noise

Manuscript received October 13, 1998; revised April 20, 1999. This work was supported by the U.K. Engineering and Physical Sciences Research Council, by Philips Research Laboratories under a CASE Studentship Award, by the Institution of Electrical Engineers under a Robinson Scholarship, by King's College London under a Junior Research Studentship Award, and by the University of York.

P. A. Dallas is with the Hellenic Aerospace Industry SA, Tanagra, Greece 32009.

J. K. A. Everard is with the Department of Electronics, The University of York, Heslington, York YO10 5DD, U.K.

Publisher Item Identifier S 0018-9480(00)00848-6.

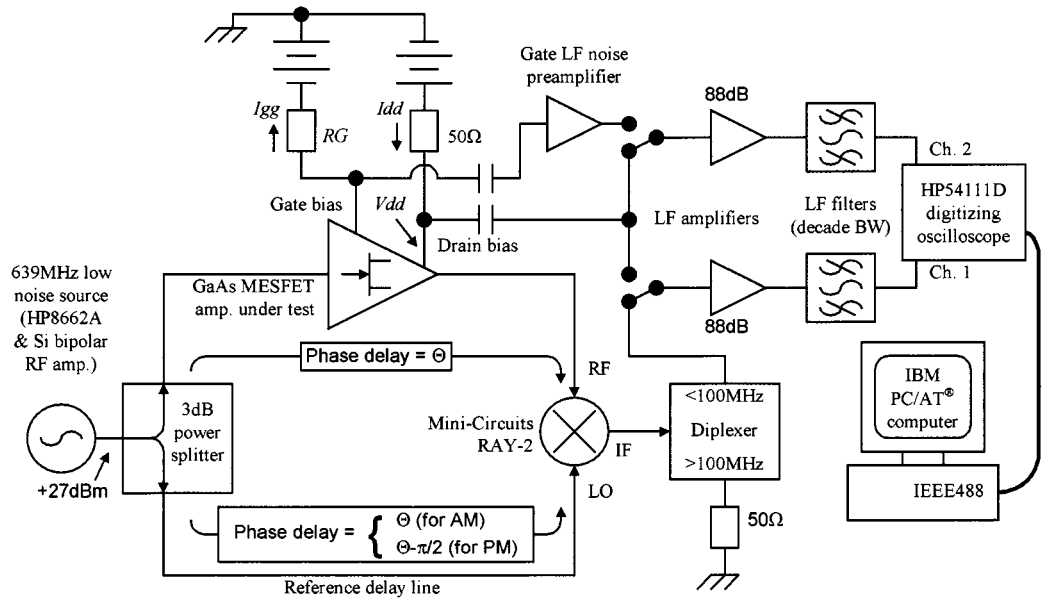

Fig. 2. Simplified block diagram of the GaAs MESFET noise measuring system. Variable attenuators (not shown) are placed at the RF input and output of the GaAs MESFET amplifier, and at the inputs of the two LF amplifiers.

TABLE I
GaAs MESFETS USED AND OPERATING CONDITIONS FOR MEASUREMENTS #1–#7. $Pout$ IS THE RF OUTPUT POWER OF THE GaAs MESFET AMPLIFIER. Rg IS THE LF GATE RESISTANCE OF THE MESFET (MEASURED AT 188.5 Hz); ∞ INDICATES THAT Rg WAS TOO HIGH TO BE MEASURED. OTHER PARAMETERS ARE DEFINED IN FIG. 2

#	MESFET	Application	Operation	*Pout*	*Vdd*	*Idd*	*-Igg*	*RG*	*Rg*
1	AT-12535	General purpose	4dB gain compression	100mW	5V	50mA	40μA	1kΩ	20kΩ
2	AT-12535	General purpose	linear	6.3mW	5V	50mA	<5μA	39kΩ	200kΩ
3	AT-12535	General purpose	4dB gain compression	105mW	5V	50mA	40μA	39kΩ	20kΩ
4	HMF-2402	Medium power	linear	42mW	7V	0.25A	5μA	3.9kΩ	∞
5	HMF-2402	Medium power	4dB gain compression	580mW	7V	0.25A	1.2mA	3.9kΩ	80Ω
6	AT-8140	Medium power	linear	36mW	7V	0.3A	10μA	3.9kΩ	∞
7	AT-8140	Medium power	4dB gain compression	620mW	7V	0.3A	350μA	3.9kΩ	1kΩ

on the gate terminal of the GaAs MESFET, and the cross-correlation coefficients between all of the drain LF, gate LF, and modulation noises.

Fig. 2 shows a block diagram of the measuring system. The measuring system uses the GaAs MESFET under test in an amplifier rather than in an oscillator, as this simplifies the construction of the equipment and the acquisition and interpretation of the results.

A 639-MHz sinusoidal signal (the "RF carrier") from a low-noise source is fed to the GaAs MESFET amplifier under test. The signal on the output of the amplifier is mixed with a sample of the original 639-MHz signal, demodulating the AM noise when the inputs of the mixer are in phase, and the PM noise when they are in quadrature.

The GaAs MESFET amplifier used originally had low Q matching networks. These were found to be too dispersive, with the result that the reference delay line in the phase bridge only offered a poor approximation to the network phase response. It was, therefore, decided to dispense with the matching networks altogether, and to feed and load the MESFET resistively.

The measuring system includes low-noise amplifiers, which amplify the LF noise on the gate and drain terminals of the GaAs MESFET under test. By appropriate connection of the LF amplifiers (the connections are shown as switches in Fig. 2), the system can be set to simultaneously sample any two of the LF drain noise, LF gate noise, and the demodulated AM or PM noise. A separate preamplifier is used to amplify the noise on the gate terminal of the GaAs MESFET under test. This consists of two cascaded common-emitter BC559 silicon bipolar transistors; these are ordinary p-n-p low-noise audio devices, with a noise figure of 1.2 dB and a flicker corner at approximately 30 Hz.

III. SIGNAL PROCESSING

The two noise signals detected by the measuring system are sampled simultaneously and stored by an HP54111D digitizing oscilloscope. The samples are then filtered digitally and also passed through a digital notch filter that removes power-line hum components. After digital filtering, the power spectral densities of the two noise signals and the cross-correlation coefficient between the two are calculated.

IV. EXPERIMENTAL RESULTS

Measurements have been taken on a small sample of GaAs MESFET's in order to investigate the capabilities of the measuring system. The characteristics of the devices and operating conditions are summarized in Table I.

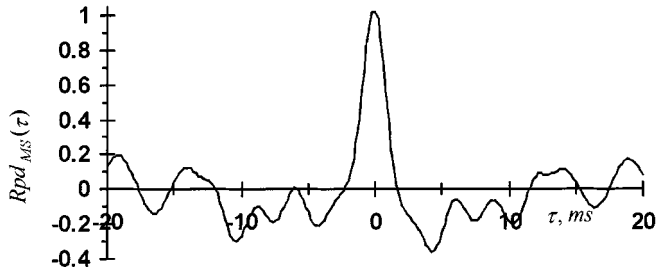

Fig. 3. Cross-correlation coefficient for noise from 40 to 400 Hz between the measured PM and LF drain noises of an AT-12 535 GaAs MESFET (from measurement #3).

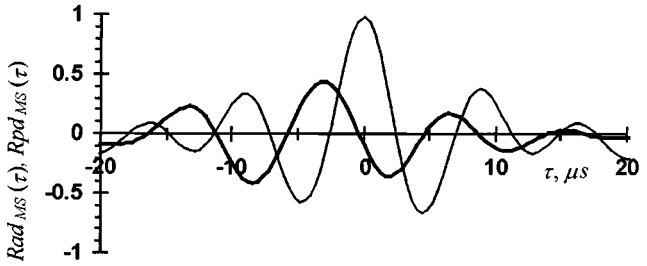

Fig. 4. Measured cross-correlation coefficients $Rpd_{MS}(\tau)$ (wide line) and $\mathrm{Rad}_{MS}(\tau)$ (narrow line) for the 20–100-kHz range (from measurement #5).

A typical cross correlation versus τ is shown in Fig. 3. The noise spectral densities (double-sided spectra) measured are shown in Figs. 5–8. Tables II–VI give the peak values of the magnitudes of the cross-correlation coefficients $\mathrm{Rad}_{MS}(\tau), Rpd_{MS}(\tau)$, $Rag_{MS}(\tau)$, $Rpg_{MS}(\tau)$, and $Rdg_{MS}(\tau)$ measured between the AM and LF drain, PM and LF drain, AM and LF gate, PM and LF gate, and LF drain and LF gate noises, respectively (τ is the time delay between measurands in the cross-correlation function).

Separate measurements were taken over overlapping decade-wide bandwidths, defined by the analog "LF filter" blocks shown in Fig. 2. This was done primarily to avoid excessive weighting of the cross-correlation coefficients by the stronger lower frequency components. Splitting the observed spectrum into decades also makes it possible to at least coarsely account for the variation of GaAs MESFET parameters (mainly gd) with frequency [25] in the calculations shown later in this paper.

A problem arises due to the cable, component, and parasitic capacitances in the GaAs MESFET amplifier gate circuit. These form a parallel *R-C* network with RG and the LF gate admittance of the GaAs MESFET, which attenuates the gate LF noise at higher frequencies and also introduces a phase delay. The suffix "§" in Tables IV–VI shows that this phase delay exceeds 10°; this has been chosen arbitrarily as the delay beyond which the cross-correlation coefficient is considered to be inaccurate.

Cross-correlation coefficients not marked with the suffix "§" had their peak value at $|\tau|$ no greater than two sample periods of the digitizing oscilloscope.[1] The only exception to this was $Rpd_{MS}(\tau)$ for measurement #5, for the 20–100-kHz frequency range. This was measured six times and, in all six measurements, $Rpd_{MS}(\tau)$ was found to consistently peak with the PM noise, leading the LF drain noise by 5–7 samples (i.e., at $\tau \approx -3\ \mu$s). Interestingly, $\mathrm{Rad}_{MS}(\tau)$ did not exhibit this characteristic (see Fig. 4).

A. Modulation and LF Drain Noise Cross Correlation

When the GaAs MESFET's tested were driven into 4-dB gain compression, a value commonly used in oscillators, it was found that, in most cases, the cross-correlation coefficients $|\mathrm{Rad}_{MS}|$ and $|Rpd_{MS}|$ approached 100%. This indicates that, in these instances, the AM and PM noise was almost exclusively due to modulation of LF noise. Such high levels of correlation were not encountered when the GaAs MESFET's were operated in their linear region. The measured cross-correlation coefficients in this case varied substantially between devices, making it difficult to draw any general conclusions, especially as the number of devices tested was small.

[1]The oscilloscope sampling rate was either 20 or 25 times the highest frequency in every range.

B. Gate LF Noise Cross-Correlation Coefficients

The LF noise potential that affects the gate depletion region width and, hence, the drain current and gate nonlinearities of the GaAs MESFET under test, is not the potential measured (relative to the source terminal) on the gate terminal of the MESFET, but the distributed potential across the gate depletion region caused by the gate flicker noise sources (eg andig in Fig. 1). Rag_{MS}, Rpg_{MS}, and Rdg_{MS} are, therefore, not direct measures of the relation between the LF noise generated in the gate depletion region of the MESFET and the modulation and LF drain noises. Nevertheless, Rag_{MS}, Rpg_{MS}, and Rdg_{MS} do convey useful information, and can be used indirectly for calculating the contribution of the LF noise generated in the gate depletion region to the LF drain and close-to-carrier sideband noises. This calculation is shown later.

V. Compensating the Results for the Effects of Measuring System Noise

Noise from the measuring system itself appears on all measurands, and can significantly affect the results obtained. This section shows how the results of the measurements can be compensated for the effects of measuring system noise, to give the true values of the GaAs MESFET noise levels and cross-correlation coefficients. This technique could be used for extracting the true MESFET noise parameters from measurements significantly affected by measuring system noise. In our measurements though, it has been used primarily as a means of demonstrating that the measuring system noise has a negligible effect on the accuracy of the measured parameters.

A. Determining the Conversion Sensitivity Values

Discussion

The GaAs MESFET under test will convert one form of noise to another. This behavior is accounted for, to first order, by defining a set of real-valued frequency-independent conversion sensitivity values that describe this. The set has been expanded to include the LF gain of the MESFET (kdg, kgd) and the FM

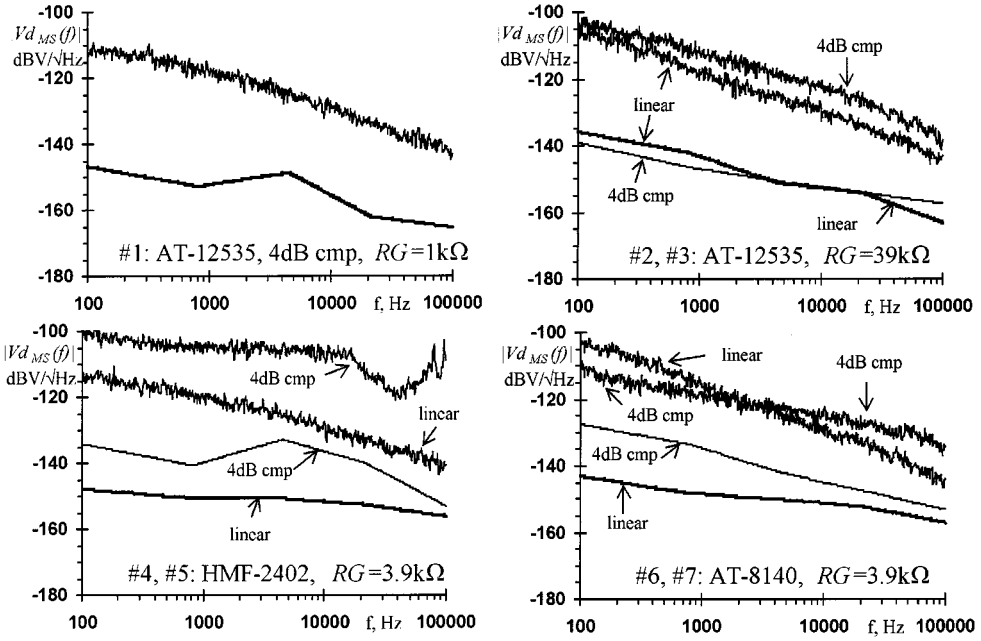

Fig. 5. LF drain terminal noise voltage spectral densities. The upper (noisy) traces in each plot are the measured LF drain terminal noise voltages $|Vd_{MS}(f)|$, and the solid lines show the calculated measuring system noise floor $|Vd_{SY}(f)|$.

discriminator action of the phase bridge (kaf, kpf, kgf, kdf) (see Table VII). The sensitivities to LF gate noise and LF drain noise are determined by injecting a low-level ($\cong 50$ μV rms) LF sinusoidal signal on the respective bias port of the GaAs MESFET amplifier and observing the resulting signal on the measurand. The sensitivities to AM and FM noise are determined by applying small amounts of AM and FM on the 639-MHz source.

B. Determining the Measuring System Noise Floor

As the levels of the measurands are small, the measuring system noise floor has to be determined as accurately as possible. This could be measured by removing the GaAs MESFET amplifier and replacing it with a transmission line of equal electric length in the phase bridge; cooled resistors could be connected across the bias supplies to simulate the resistance the MESFET presents to the LF amplifiers. This method may be inaccurate though, as it does not account for noise reaching the measurands indirectly through LF gain, modulation, and detection by the GaAs MESFET under test. Instead, the measuring system noise floor has been calculated by summing the power spectral densities of all noise contributions from the measuring system components, whether these contribute to the measurands directly or indirectly. The appropriate conversion sensitivity values have been used to determine the effect of noise sources reaching a measurand indirectly. The measuring system noise calculated thus is shown as a solid line in Figs. 5–8. Fig. 6 also shows the noise measured with the GaAs MESFET amplifier removed, with a resistor (at room temperature) of value equal to the resistance presented by the MESFET gate (Rg in Table I, open circuit for $Rg = \infty$) in place of the GaAs MESFET amplifier gate bias port.

C. Statistical Average Function Definition

- Noise level (variance): The power level of our time-limited sample set$x(t)$ is simply its statistical variance

$$\sigma^2 x = \frac{1}{T} \cdot \int_0^T |x(t)|^2 \, dt$$

where T is the sampling duration. The frequency-domain equivalent of this is [26, p. 85]

$$\sigma^2 x = \frac{1}{T} \cdot \int_{-\infty}^{\infty} |x(f)|^2 \, df. \tag{1}$$

- Cross correlation and covariance: The cross-correlation coefficient $Rxy(\tau)$ between two sample sets $x(t)$ and $y(t)$ is defined as[2]

$$Rxy(\tau) = \frac{\frac{1}{T} \cdot \int_0^T x(t)^* \cdot y(t+\tau) \, dt}{\sqrt{\sigma^2 x \cdot \sigma^2 y}}$$

with one notable exception (20–100 kHz $Rpd_{MS}(\tau)$ for measurement #5), in the GaAs MESFET noise measurements taken, the peaks of the cross-correlation coefficients were found to be at $\tau \approx 0$. In this analysis, the effects of offset τ will be assumed to be negligible,[3] and the peak Rxy of the cross-correlation coefficient will be taken to be at $\tau = 0$

$$Rxy = Rxy(0).$$

[2]In the usual definition of the cross-correlation coefficient, the mean values are subtracted from the two time-domain variables in the integration before they are multiplied. This operation is not shown here to avoid unnecessary algebra.

[3]The consequences of this approximation could be significant, and should be checked in future work.

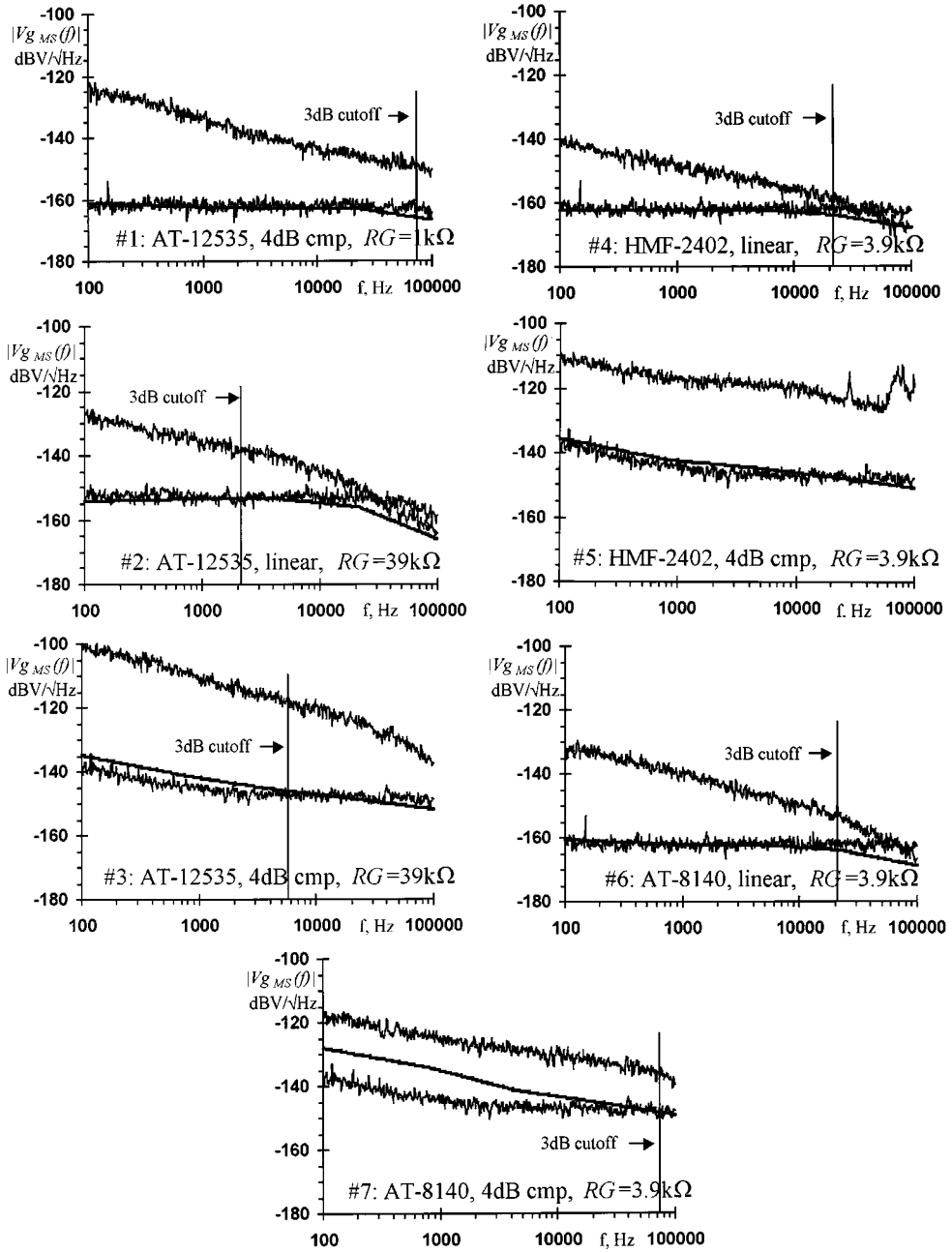

Fig. 6. LF gate terminal noise voltage spectral densities. The upper trace is the measured LF gate terminal noise $|Vg_{MS}(f)|$, and the lower trace is the measuring system noise, measured with the GaAs MESFET under test replaced by a resistor approximately equal to Rg. The solid line represents the calculated measuring system noise floor $|Vg_{SY}(f)|$. The 3-dB cutoff frequency is the upper cutoff of the *R-C* network formed by RG, the cable and circuit capacitances, and the MESFET gate LF admittance. For measurement #5, this cutoff frequency is off the scale (at 1.00 MHz).

For notational brevity, the covariance $Sxy(\tau)$ (with $\tau = 0$) will be used in place of the cross-correlation coefficient. This is

$$Sxy = Rxy \cdot \sqrt{\sigma^2 x \cdot \sigma^2 y}$$
$$\therefore Sxy = \frac{1}{T} \cdot \int_0^T x(t)^* \cdot y(t)\, dt. \tag{2}$$

The frequency-domain equivalent of this is [27, pp. 203–206]

$$Sxy = \frac{1}{T} \cdot \int_{-\infty}^{\infty} x(f)^* \cdot y(f)\, df. \tag{3}$$

D. Compensating the GaAs MESFET Noise Variance

Noise from the components of the measuring system is not correlated with the noise generated by the GaAs MESFET under test. The variance (power level) of the noise generated by the GaAs MESFET under test itself, i.e., $\sigma^2 x$, can, therefore, be determined by subtracting the measuring system noise floor $\sigma^2 x_{SY}$ from the total measured power level $\sigma^2 x_{MS}$

$$\sigma^2 x = \sigma^2 x_{MS} - \sigma^2 x_{SY}.$$

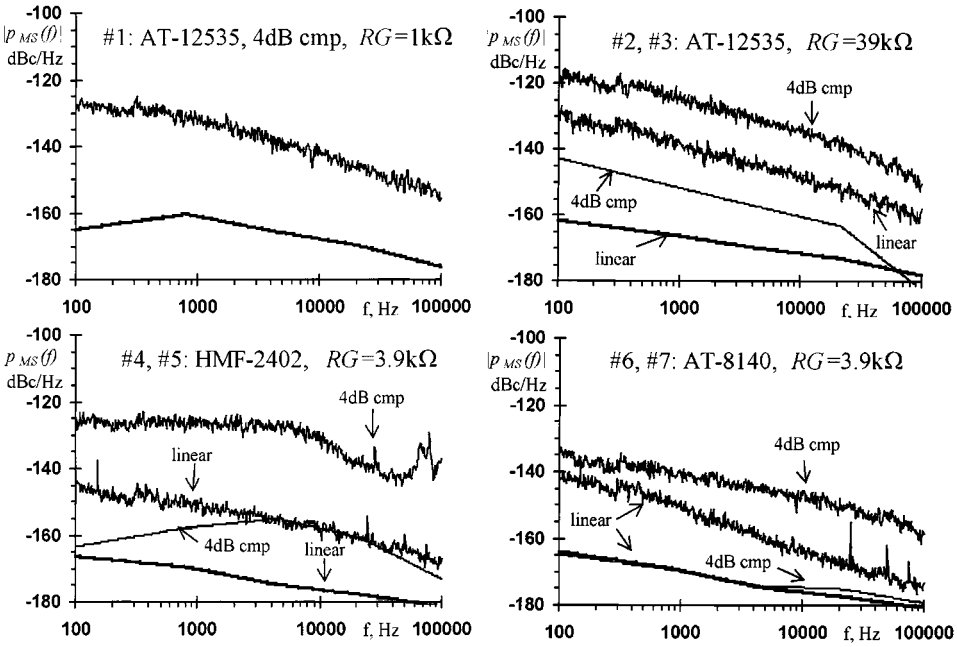

Fig. 7. Single-sideband PM noise power spectral densities. The upper (noisy) traces in each plot are the measured single-sideband PM noises $|p_{MS}(f)|$, and the solid lines show the calculated measuring system noise floor $|p_{SY}(f)|$.

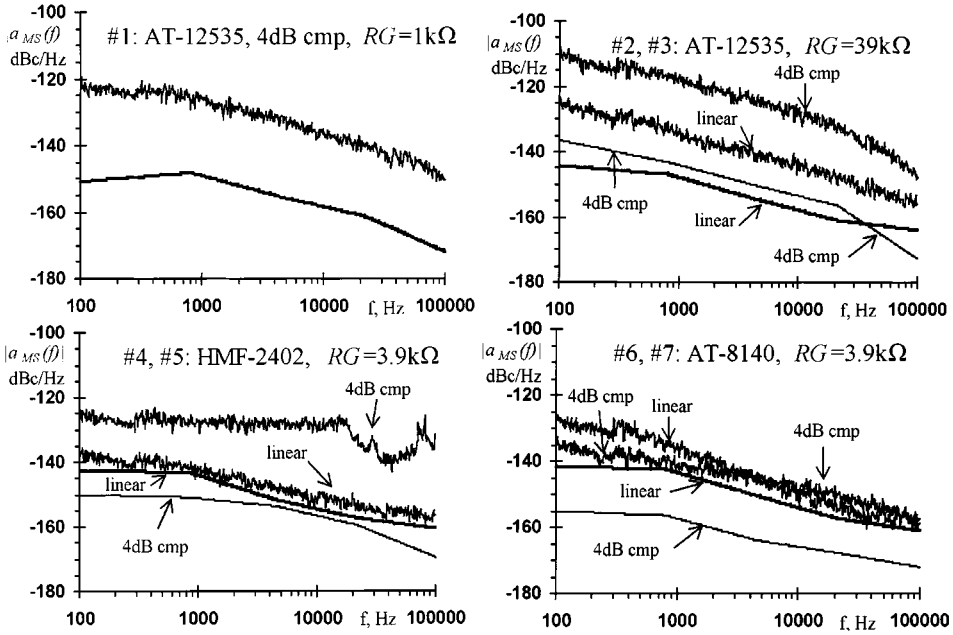

Fig. 8. Single-sideband AM noise power spectral densities. The upper (noisy) traces in each plot are the measured single-sideband AM noises $|a_{MS}(f)|$, and the solid lines show the calculated measuring system noise floor $|a_{SY}(f)|$.

E. Compensating the Covariance Values

The covariance values between the PM, AM, LF gate, and LF drain noises actually generated by the GaAs MESFET under test itself can be calculated from information provided by the measuring system. The derivation of the covariance Spd (its peak value) between the PM and LF drain noises is shown here; all other covariances can be determined using the same approach.

The PM noise $p(f)$ imposed on the amplified RF carrier by the GaAs MESFET under test consists of two components $p_c(f)$, which is correlated with the correlated part of the LF

TABLE II
$|\mathrm{Rad}_{MS}|$: PEAK MAGNITUDE OF THE CROSS-CORRELATION COEFFICIENT BETWEEN THE MEASURED AM AND LF DRAIN NOISES FOR MEASUREMENTS #1–#7

	Frequency range, Hz				
#	40-400	200-2k	1k-10k	4k-40k	20k-100k
1	93%	94%	95%	95%	94%
2	11%	9%	37%	51%	45%
3	99%	99%	99%	99%	99%
4	29%	20%	26%	34%	35%
5	95%	97%	98%	98%	98%
6	80%	78%	73%	69%	43%
7	93%	96%	97%	97%	93%

TABLE III
$|Rpd_{MS}|$: PEAK MAGNITUDE OF THE CROSS–CORRELATION COEFFICIENT BETWEEN THE MEASURED PM AND LF DRAIN NOISES FOR MEASUREMENTS #1–#7

	Frequency range, Hz				
#	40-400	200-2k	1k-10k	4k-40k	20k-100k
1	92%	93%	93%	92%	90%
2	9%	10%	37%	48%	46%
3	98%	98%	98%	98%	97%
4	20%	17%	19%	32%	33%
5	56%	78%	82%	60%	44%
6	83%	79%	70%	59%	44%
7	93%	96%	97%	97%	96%

TABLE IV
$|Rpd_{MS}|$: PEAK MAGNITUDE OF THE CROSS-CORRELATION COEFFICIENT BETWEEN THE MEASURED AM AND LF GATE NOISES FOR MEASUREMENTS #1–#7

	Frequency range, Hz				
#	40-400	200-2k	1k-10k	4k-40k	20k-100k
1	68%	67%	65%	59%§	63%§
2	36%§	31%§	27%§	25%§	25%§
3	98%	97%§	96%§	96%§	93%§
4	13%	11%	12%§	20%§	19%§
5	13%	10%	19%	39%	41%
6	58%	64%	63%§	53%§	24%§
7	53%	64%	76%	81%§	81%§

TABLE V
$|Rpd_{MS}|$: PEAK MAGNITUDE OF THE CROSS–CORRELATION COEFFICIENT BETWEEN THE MEASURED PM AND LF GATE NOISES FOR MEASUREMENTS #1–#7

	Frequency range, Hz				
#	40-400	200-2k	1k-10k	4k-40k	20k-100k
1	71%	70%	64%	64%§	66%§
2	34%§	35%§	30%§	25%§	25%§
3	96%	95%§	93%§	93%§	92%§
4	45%	40%	41%§	40%§	34%§
5	30%	28%	20%	10%	63%
6	8%	13%	17%§	12%§	10%§
7	49%	64%	76%	81%§	84%§

TABLE VI
$|Rpd_{MS}|$: PEAK MAGNITUDE OF THE CROSS-CORRELATION COEFFICIENT BETWEEN THE MEASURED LF DRAIN AND LF GATE NOISES FOR MEASUREMENTS #1–#7

	Frequency range, Hz				
#	40-400	200-2k	1k-10k	4k-40k	20k-100k
1	58%	60%	51%	50%§	53%§
2	7%§	8%§	20%§	22%§	19%§
3	94%	92%§	89%§	88%§	89%§
4	12%	11%	8%§	12%§	17%§
5	12%	13%	13%	24%	27%
6	19%	36%	59%§	62%§	56%§
7	74%	82%	89%	92%§	93%§

drain noise generated by the MESFET, and $p_u(f)$, which is uncorrelated with the LF drain noise. $p(f)$ is

$$p(f) = p_c(f) + p_u(f).$$

The LF drain noise $Vd(f)$ generated by the GaAs MESFET under test consists of two components $Vd_c(f)$, which is correlated with $p_c(f)$, and $Vd_u(f)$, which is not. $Vd(f)$ is

$$Vd(f) = Vd_c(f) + Vd_u(f). \tag{4}$$

TABLE VII
NOISE LEVELS: CORRELATIONS AND COVARIANCES FROM MEASUREMENT #3. THE MEASURED VALUES ($_{MS}$ SUBSCRIPT) ARE SHOWN

Sensitivity of measurand...	a_{MS}	p_{MS}	Vg_{MS}	Vd_{MS}
...to AM noise:	*kaa*	*kpa*	*kga*	*kda*
...to FM noise:	*kaf*	*kpf*	*kgf*	*kdf*
...to gate LF noise:	*kag*	*kpg*	1	*kdg*
...to drain LF noise:	*kad*	*kpd*	*kgd*	1

Assuming an approximately linear and frequency-independent conversion of LF drain noise to PM noise, the conversion sensitivity value kpd can be used to give $p_c(f)$ as a function of $Vd_c(f)$

$$\begin{aligned} p_c(f) &= Vd_c(f) \cdot kpd \\ \therefore\ p(f) &= Vd_c(f) \cdot kpd + p_u(f) \end{aligned} \tag{5}$$

The peak of the covariance between the PM and LF drain noises Spd is, per (3),

$$Spd = \frac{1}{T} \cdot \int_{-\infty}^{\infty} p(f)^* \cdot Vd(f)\ df$$

with (1), (4), and (5), provided T is long enough for the uncorrelated components to integrate out, this becomes

$$Spd = \frac{1}{T} \cdot \int_{-\infty}^{\infty} |Vd_c(f)|^2 \cdot kpd\ df \Rightarrow Spd = \sigma^2 Vd_c \cdot kpd \tag{6}$$

(as kpd is real-valued and frequency-independent).

The measured PM noise $p_{MS}(f)$ contains $p(f)$, and also noise from the measuring system. The measuring system noise sources affecting $p_{MS}(f)$ can be split into the following two categories:

- $p_{uSY}(f)$, these which contribute to the PM noise measurand, but not to the LF drain noise measurand.
- Measuring system sources of AM noise $a_{cSY}(f)$, FM noise $f_{cSY}(f)$, LF noise on the gate $Vg_{cSY}(f)$ and on the drain $Vd_{cSY}(f)$, which contribute to both the PM noise and LF drain noise measurands either directly or indirectly.

Using (5) for $p(f)$ in $p_{MS}(f)$, $p_{MS}(f)$ is expressed as

$$\begin{aligned} p_{MS}(f) = \Big\{ & Vd_c(f) \cdot kpd + p_u(f) + \Sigma p_{uSY}(f) \\ & + \Sigma[a_{cSY}(f) \cdot c_p] \cdot kpa \\ & + \Sigma[f_{cSY}(f) \cdot c_p] \cdot kpf + [\Sigma Vg_{cSY}(f) \cdot c_p] \\ & \cdot kpg + \Sigma[Vd_{cSY}(f) \cdot c_p] \cdot kpd \Big\} \end{aligned} \tag{7}$$

where Σ denotes the sum of the noises from all relevant measuring system noise sources.

Each measuring system noise source has an associated constant c_p. Normally, $c_p = 1$. For measuring system noise sources that reach $p_{MS}(f)$ through an attenuator, c_p is equal to the attenuation. Also, c_p is negative for measuring system noise sources that reach $p_{MS}(f)$ inverted (used for series noise sources). c_p is real valued.

The measured LF drain noise $Vd_{MS}(f)$ contains $Vd(f)$ and noise from the measuring system. The measuring system noise sources affecting $Vd_{MS}(f)$ are separated into

- $Vd_{uSY}(f)$, these which only contribute to the LF drain noise measurand.
- $a_{cSY}(f), f_{cSY}(f), Vg_{cSY}(f)$, and $Vd_{cSY}(f)$, which also appear in $p_{MS}(f)$.

Using (4) for $Vd(f)$

$$\begin{aligned} Vd_{MS}(f) = \Big\{ & Vd_c(f) + Vd_u(f) + \Sigma Vd_{uSY}(f) \\ & + \Sigma[a_{cSY}(f) \cdot c_d] \cdot kda + \Sigma[f_{cSY}(f) \cdot c_d] \cdot kdf \\ & + \sigma[Vg_{cSY}(f) \cdot c_d] \cdot kdg + \Sigma[Vd_{cSY}(f) \cdot c_d] \Big\} \end{aligned} \tag{8}$$

The constants c_d serve the same purpose here as constants c_p do in (7).

The peak of the measured covariance[4] Spd_{MS} between the PM and the LF drain noises is

$$Spd_{MS} = \frac{1}{T} \cdot \int_{-\infty}^{\infty} p_{MS}(f)^* \cdot Vd_{MS}(f)\, df.$$

Replacing $p_{MS}(f)$ and $Vd_{MS}(f)$ in Spd_{MS} from (7) and (8), provided T is long enough for the uncorrelated components to integrate out

$$\begin{aligned} & Spd_{MS} \\ & = \frac{1}{T} \cdot \int_{-\infty}^{\infty} \Big\{ |Vd_c(f)|^2 \cdot kpd + \Sigma[|a_{cSY}(f)|^2 \cdot c_p \cdot c_d] \\ & \qquad \cdot kpa \cdot kda + \Sigma[|f_{cSY}(f)|^2 \cdot c_p \cdot c_d] \cdot kpf \cdot kdf \\ & \qquad + \Sigma[|Vg_{cSY}(f)|^2 \cdot c_p \cdot c_d] \cdot kpg \cdot kdg \\ & \qquad + \Sigma[|Vd_{cSY}(f)|^2 \cdot c_p \cdot c_d] \cdot kpd \Big\}\, df \Rightarrow \\ & Spd_{MS} \\ & = \Big[\sigma^2 Vd_c \cdot kpd + \Sigma(\sigma^2 a_{cSY} \cdot c_p \cdot c_d) \cdot kpa \cdot kda \\ & \quad + \Sigma(\sigma^2 f_{cSY} \cdot c_p \cdot c_d) \cdot kpf \cdot kdf \\ & \quad + \Sigma(\sigma^2 Vg_{cSY} \cdot c_p \cdot c_d) \cdot kpg \cdot kdg \\ & \quad + \Sigma(\sigma^2 Vd_{cSY} \cdot c_p \cdot c_d) \cdot kpd \Big] \end{aligned}$$

This and (6) give Spd, the covariance between the actual PM and LF drain noises generated by the GaAs MESFET

$$\begin{aligned} Spd = \Big[& Spd_{MS} - \Sigma(\sigma^2 a_{cSY} \cdot c_p \cdot c_d) \cdot kpa \cdot kda \\ & - \Sigma(\sigma^2 f_{cSY} \cdot c_p \cdot c_d) \cdot kpf \cdot kdf \\ & - \Sigma(\sigma^2 Vg_{cSY} \cdot c_p \cdot c_d) \cdot kpg \cdot kdg \\ & - \Sigma(\sigma^2 Vd_{cSY} \cdot c_p \cdot c_d) \cdot kpd \Big]. \end{aligned}$$

[4]The value of the covariance can be calculated from the measured cross correlation and noise levels using (2).

VI. Calculating the Flicker Noise Source Levels and Cross Correleation

A. Basic Assumptions

The following assumptions will be made about the GaAs MESFET and its equivalent circuit:

- $id(f)$ will be assumed to be uncorrelated with $eg(f)$ and $ig(f)$, as it represents noise generated in the conducting channel and in the substrate depletion region.
- $eg(f)$ and $ig(f)$ may be partially correlated, as they are believed to both originate from the gate depletion region. $eg(f)$ and $ig(f)$ will be split into their correlated components $eg_c(f)$ and $ig_c(f)$ respectively, and uncorrelated components $eg_u(f)$ and $ig_u(f)$, respectively,

$$eg(f) = eg_c(f) + eg_u(f)$$

and

$$ig(f) = ig_c(f) + ig_u(f). \tag{9}$$

The correlated components $eg_c(f)$ and $ig_c(f)$ will be assumed to have the same frequency spectrum, and not to be delayed significantly with respect to one another, so that $eg_c(f)$ can be expressed as

$$\begin{aligned} eg_c(f) &= ig_c(f) \cdot k \\ \therefore\ eg(f) &= ig_c(f) \cdot k + eg_u(f) \end{aligned} \tag{10}$$

where k is a real-valued frequency-independent constant.

- The PM noise $p(f)$ imposed on the RF carrier amplified by the GaAs MESFET will be considered to consist of noise from the LF flicker noise sources $eg(f)$, $ig(f)$, and $id(f)$ modulated onto the carrier by GaAs MESFET nonlinearities, and also of a separate component $p_u(f)$ not related to the LF noise sources. $p_u(f)$ is uncorrelated with $eg(f)$, $ig(f)$, and $id(f)$.
- Noise from the measuring system itself will not be taken into consideration here. The variances and covariances of the GaAs MESFET noise used in this analysis are the values compensated for the effects of measuring system noise, as described in the previous section.

B. Circuit Equations

Analysis of the equivalent circuit in Fig. 1 gives (11) and (12), shown at the bottom of page 254, for the LF drain and LF gate terminal noise voltages $Vd(f)$ and $Vg(f)$, respectively. These two equations are not sufficient for deriving $eg(f)$, $ig(f)$, and $id(f)$. The additional information required has to be provided by the third parameter, which can be measured with the measuring system, the modulation noise. The PM noise has been used here; the AM noise could have been used instead.

The PM noise $p(f)$ on the RF output of the GaAs MESFET amplifier is considered to consist of the following three components.

- The gate depletion region LF flicker noise $Vg'(f)$ (see Fig. 1), modulated onto the carrier by the nonlinear behavior of the MESFET with conversion sensitivity kpg.

TABLE VIII
CONVERSION SENSITIVITIES FROM MEASUREMENT #3

Parameter	Frequency range, Hz 40-400	200-2k	Units
kgd	0.34	0.31	V/V
kga	-0.34	-0.28	V/√(W/W)
kgf	-1.4E-09	-1.7E-09	V/Hz
kdg	-0.57	-0.57	V/V
kda	0.36	0.32	V/√(W/W)
kdf	6.4E-10	6.8E-10	V/Hz
kpg	-0.11	-0.14	√(W/W)/V
kpd	-0.030	-0.044	√(W/W)/V
kpa	0.016	0.017	√(W/W)/√(W/W)
kpf	-1.9E-09	-2.7E-09	√(W/W)/Hz

TABLE IX
SIMULTANEOUS PM–LF DRAIN NOISE MEASUREMENT MEASURING SYSTEM NOISE CONTRIBUTIONS FOR MEASUREMENT #3

Parameter	Frequency range, Hz 40-400	200-2k	Units
$\sigma^2 p_{SY}$	-145	-151	dBc/Hz
$\sigma^2 Vd_{SY}$	$(86)^2$	$(48)^2$	$(nV/\sqrt{Hz})^2$
$\Sigma(\sigma^2 a_{cSY}\cdot c_p\cdot c_d)$	2.8E-15	2.1E-15	(W/Hz)/W
$\Sigma(\sigma^2 f_{cSY}\cdot c_p\cdot c_d)$	3.2E-07	8.1E-07	Hz^2/Hz
$\Sigma(\sigma^2 Vg_{cSY}\cdot c_p\cdot c_d)$	$(9.0)^2$	$(9.0)^2$	$(nV/\sqrt{Hz})^2$
$\Sigma(\sigma^2 Vd_{cSY}\cdot c_p\cdot c_d)$	$(0.62)^2$	$(0.48)^2$	$(nV/\sqrt{Hz})^2$

- The drain LF flicker noise $Vd(f)$, modulated onto the carrier by the nonlinear behavior of the MESFET with conversion sensitivity kpd.
- Noise $p_u(f)$ not connected with the LF flicker noise sources.

$p(f)$ is, therefore,

$$p(f) = Vg'(f)\cdot kpg + Vd(f)\cdot kpd + p_u(f).$$

Replacing $Vg'(f)$ and $Vd(f)$ in this with the appropriate circuit equations gives (13), shown at the bottom of the following page.

C. The Variances of and Covariances Between $Vd(f)$, $Vg(f)$, and $p(f)$

These are determined as per (1) and (3). However, they cannot be evaluated analytically with frequency-dependent (trans)admittances $Y2(f), yg(f)\cdots ym(f)$ and arbitrary frequency-dependent noise sources $ig(f)$, $eg(f)$, and $id(f)$. The (trans)admittances have to be assumed to be independent of frequency at the flicker noise frequencies.[5] They can then be moved outside the frequency integrals, leaving only the noise sources within the integrals.

In practical terms, this makes it necessary to split the frequency range considered into a number of relatively narrow frequency bands, over which this approximation is valid. We split the frequency range into overlapping decades, and found the (trans)admittances typically changed by less than 1.1:1 between adjacent decades. The largest variation recorded was 1.62:1; however, larger variations have been reported elsewhere [25].

As the (trans)admittances $Y2(f), yg(f)\cdots ym(f)$ are not to be functions of frequency, their imaginary parts (susceptances) have been set to zero, leaving just the (trans)conductances $G2, gg\cdots gm$. At flicker noise frequencies in the hertz and kilohertz regions, this is not an unrealistic approximation, especially in cases where the MESFET gate is driven with a large RF signal and exhibits significant conductance.

[5]This is a significant assumption; its validity and its effect on the accuracy of the results obtained should be checked in future work.

TABLE X
SIMULTANEOUS LF DRAIN–LF GATE NOISE MEASUREMENT MEASURING SYSTEM NOISE CONTRIBUTIONS FOR MEASUREMENT #3

Parameter	Frequency range, Hz 40-400	200-2k	Units
$\sigma^2 Vd_{SY}$	$(131)^2$	$(66)^2$	$(nV/\sqrt{Hz})^2$
$\sigma^2 Vg_{SY}$	$(145)^2$	$(86)^2$	$(nV/\sqrt{Hz})^2$
$\Sigma(\sigma^2 a_{cSY}\cdot c_d\cdot c_g)$	2.8E-15	2.1E-15	(W/Hz)/W
$\Sigma(\sigma^2 f_{cSY}\cdot c_d\cdot c_g)$	3.2E-07	8.1E-07	Hz^2/Hz
$\Sigma(\sigma^2 Vg_{cSY}\cdot c_d\cdot c_g)$	$(9.0)^2$	$(9.0)^2$	$(nV/\sqrt{Hz})^2$
$\Sigma(\sigma^2 Vd_{cSY}\cdot c_d\cdot c_g)$	$(0.52)^2$	$(0.42)^2$	$(nV/\sqrt{Hz})^2$

TABLE XI
NOISE LEVELS: CORRELATIONS AND COVARIANCES FROM MEASUREMENT #3. THE MEASURED VALUES (MS SUBSCRIPT) AND THE VALUES COMPENSATED FOR THE EFFECTS OF MEASURING SYSTEM NOISE (NO SUBSCRIPT) ARE SHOWN

Parameter	Frequency range, Hz 40-400	200-2k	Units
$\sigma^2 p_{MS}$	-121	-123	dBc/Hz
$\sigma^2 p$	-121	-123	dBc/Hz
$\sigma^2 Vd_{MS}$	$(4.6)^2$	$(2.9)^2$	$(\mu V/\sqrt{Hz})^2$
$\sigma^2 Vd$	$(4.6)^2$	$(2.9)^2$	$(\mu V/\sqrt{Hz})^2$
$\sigma^2 Vg_{MS}$	$(5.7)^2$	$(3.5)^2$	$(\mu V/\sqrt{Hz})^2$
$\sigma^2 Vg$	$(5.7)^2$	$(3.5)^2$	$(\mu V/\sqrt{Hz})^2$
Rpd_{MS}	98	98	%
Spd_{MS}	3.9E-12	1.9E-12	√[(W/Hz)/W]·V/√Hz
Spd	3.9E-12	1.9E-12	√[(W/Hz)/W]·V/√Hz
Rdg_{MS}	-94	-92	%
Sdg_{MS}	-2.5E-11	-9.3E-12	V/√Hz·V/√Hz
Sdg	-2.5E-11	-9.3E-12	V/√Hz·V/√Hz

TABLE XII
MEASURING SYSTEM AND GAAS MESFET (TRANS)CONDUCTANCES FOR MEASUREMENT #3. THE PARAMETERS ARE DEFINED IN FIG. 1. THEY ARE CONSIDERED TO BE REAL VALUED, SO THAT $Y1 = G1$, $Y2 = G2, YG = GG$, ETC.

Parameter	Frequency range, Hz 40-400	200-2k	Units
1/*G1*	24	24	Ω
1/*G2*	35	35	kΩ
1/*gg*	170	120	kΩ
1/*gf*	57	60	kΩ
gm	26	27	mS
1/*gd*	140	100	Ω

With these simplifying assumptions, using simple algebraic manipulations, the variances $\sigma^2 Vd$, $\sigma^2 Vg$, and$\sigma^2 p$ of $Vd(f)$, $Vg(f)$, and $p(f)$, and the covariances Sdg between $Vd(f)$ and $Vg(f)$, and Spd from $p(f)$ to $Vd(f)$ can be derived using (1), (3), (9)–(13). They are expressed as functions of constant k from (10), and of the variances $\sigma^2 eg, \sigma^2 id, \sigma^2 ig_c, \sigma^2 ig$, and $\sigma^2 p_u$ of $eg(f)$, $id(f)$, $ig_c(f)$, $ig(f)$, and $p_u(f)$, respectively.

D. Solving for the Noise Source Levels

The equations for $\sigma^2 Vd, \sigma^2 Vg$, $\sigma^2 p, Sdg$, and Spd contain sufficient information for calculating the levels of noise sourceseg, ig and id, the level of the uncorrelated PM noise p_u, and the cross-correlation coefficient (its peak value) from eg to ig.

The equations for $\sigma^2 Vd, \sigma^2 Vg, Sdg$, and Spd form a system of simultaneous equations, with the four unknowns $\sigma^2 eg, \sigma^2 id$, $\sigma^2 ig_c \cdot k$, and $\sigma^2 ig$; (14)–(16), shown at the bottom of this page, and (17), shown at the bottom of the following page, are the solutions of this system. The results obtained from these equations can be used with the measured value of $\sigma^2 p$ to calculate the

$$Vd(f) = \frac{eg(f)\cdot Y2(f)\cdot\Big[yf(f)-ym(f)\Big]-id(f)\cdot\Big[Y2(f)+yg(f)+yf(f)\Big]-ig(f)\cdot\Big[yf(f)-ym(f)\Big]}{\Big[Y1(f)+yd(f)\Big]\cdot\Big[Y2(f)+yg(f)\Big]+yf(f)\cdot\Big[Y1(f)+yd(f)+Y2(f)+yg(f)+ym(f)\Big]} \tag{11}$$

$$Vg(f) = \frac{\begin{array}{l}-eg(f)\cdot\Big\{yf(f)\cdot\Big[yg(f)+ym(f)\Big]+\Big[Y1(f)+yd(f)\Big]\cdot\Big[yf(f)+yg(f)\Big]\Big\}\\ -id(f)\cdot yf(f)-ig(f)\cdot\Big[Y1(f)+yd(f)+yf(f)\Big]\end{array}}{\Big[Y1(f)+yd(f)\Big]\cdot\Big[Y2(f)+yg(f)\Big]+yf(f)\cdot\Big[Y1(f)+yd(f)+Y2(f)+yg(f)+ym(f)\Big]} \tag{12}$$

$$p(f) = \frac{\begin{array}{l}eg(f)\cdot\Big\{kpg\cdot\Big[Y1(f)+yd(f)+yf(f)\Big]+kpd\cdot\Big[yf(f)-ym(f)\Big]\Big\}\cdot Y2(f)\\ -id(f)\cdot\Big\{kpg\cdot yf(f)+kpd\cdot\Big[Y2(f)+yg(f)+yf(f)\Big]\Big\}\\ -ig(f)\cdot\Big\{kpg\cdot\Big[Y1(f)+yd(f)+yf(f)\Big]+kpd\cdot\Big[yf(f)-ym(f)\Big]\Big\}\end{array}}{\Big[Y1(f)+yd(f)\Big]\cdot\Big[Y2(f)+yg(f)\Big]+yf(f)\cdot\Big[Y1(f)+yd(f)+Y2(f)+yg(f)+ym(f)\Big]}+p_u(f) \tag{13}$$

$$\sigma^2 eg = \sigma^2 Vg + \frac{\begin{array}{l}\sigma^2 Vd\cdot\Big\{kpg\cdot gf\cdot(G1+gd+gf)-kpd\cdot\Big[(G1+gd)\cdot(G2+gg)+gf\cdot(G1+gd+G2+gg+gm)\Big]\Big\}\\ -Sdg\cdot kpg\cdot 2\cdot(G1+gd+gf)\cdot(G2+gg+gf)\\ +Spd\cdot\Big[(G1+gd)\cdot(G2+gg)+gf\cdot(G1+gd+G2+gg+gm)\Big]\end{array}}{kpg\cdot(gf-gm)\cdot(G2+gg+gf)} \tag{14}$$

$$\sigma^2 id = \frac{\begin{array}{l}\sigma^2 Vd\cdot\Big[kpd\cdot(gf-gm)+kpg\cdot(G1+gd+gf)\Big]\cdot\Big[(G1+gd)\cdot(G2+gg)+gf\cdot(G1+gd+G2+gg+gm)\Big]\\ -Spd\cdot(gf-gm)\cdot\Big[(G1+gd)\cdot(G2+gg)+gf\cdot(G1+gd+G2+gg+gm)\Big]\end{array}}{kpg\cdot(G2+gg+gf)} \tag{15}$$

$$\sigma^2 ig_c\cdot k = \frac{\begin{array}{l}\sigma^2 Vd\cdot\Big\{kpd\cdot(gf+gg)\cdot\Big[(G1+gd)\cdot(G2+gg)+gf\cdot(G1+gd+G2+gg+gm)\Big]\\ \qquad +kpg\cdot G2\cdot gf\cdot(G1+gd+gf)\Big\}\\ +\sigma^2 Vg\cdot kpg\cdot G2\cdot(gf-gm)\cdot(G2+gg+gf)\\ -Sgd\cdot kpg\cdot(G2+gg+gf)\cdot\Big[(G1+gd+gf)\cdot(G2-gg-gf)+gf\cdot(gf-gm)\Big]\\ -Spd\cdot(gf+gg)\cdot\Big[(G1+gd)\cdot(G2+gg)+gf\cdot(G1+gd+G2+gg+gm)\Big]\end{array}}{kpg\cdot(gf-gm)\cdot(G2+gg+gf)} \tag{16}$$

variance $\sigma^2 p_u$ of the uncorrelated PM noise using (18), shown at the bottom of this page.

The rms levels of the equivalent flicker noise sources eg, ig, and id are simply the square roots of their variances $\sigma^2 eg, \sigma^2 ig$ and $\sigma^2 id$, respectively. The PM noise the GaAs MESFET generates that is not due to these flicker noise sources is $\sigma^2 p_u$.

E. The Cross Correlation Between eg and ig

The covariance S between the noise sources eg and ig is, per (3),

$$S = \frac{1}{T} \cdot \int_{-\infty}^{\infty} eg(f)^* \cdot ig(f)\, df.$$

Replacing $eg(f)$ and $ig(f)$ with their expansions from (9) and (10) gives

$$S = \frac{1}{T} \cdot \int_{-\infty}^{\infty} \Big[ig_c(f) \cdot k + eg_u(f)\Big]^* \cdot \Big[ig_c(f) + ig_u(f)\Big]\, df.$$

Expanding this and deleting the uncorrelated terms that integrate to zero leaves

$$S = \frac{1}{T} \cdot \int_{-\infty}^{\infty} |ig_c(f)|^2\, df \cdot k$$

which, as per (1), is

$$S = \sigma^2 ig_c \cdot k.$$

The cross-correlation coefficient between eg and ig is then, using (2),

$$R = \frac{\sigma^2 ig_c \cdot k}{\sqrt{\sigma^2 eg \cdot \sigma^2 ig}} \tag{19}$$

with $\sigma^2 ig_c \cdot k$ from (16) and $\sigma^2 eg$ and $\sigma^2 ig$ from (14) and (17), respectively.

VII. Worked Example

An example is provided here to demonstrate the use of the procedures for calculating the GaAs MESFET flicker noise parameters. The parameters required for the equations were taken from measurement #3; they are shown in Tables VIII–XII

The GaAs MESFET (trans)conductances shown in Table XII were derived from measurements of the LF drain–source and gate–source ac resistances, and from the forward and reverse LF gains of the GaAs MESFET under test. These measurements were taken with the MESFET operating under the same conditions as for the noise measurements.

Equation (18) gives the total PM noise $\sigma^2 p$ in terms of $\sigma^2 p_u$, $\sigma^2 eg$, $\sigma^2 ig$, $\sigma^2 ig_c \cdot k$, and $\sigma^2 id$. Separating the gate flicker noise sources and drain flicker noise source gives (20) and (21), shown at the bottom of this page, which give the contribution $\sigma^2 p_g$ of the gate flicker noise sources to $\sigma^2 p$, and the contribution $\sigma^2 p_d$ of the drain flicker noise source $\sigma^2 id$ to $\sigma^2 p$. The results, shown in Table XIV, indicate that, in this case, the PM noise is caused almost exclusively by the gate flicker noise sources.

$$\sigma^2 ig = \frac{\begin{array}{l} -\sigma^2 Vd \cdot \left\{ \begin{array}{l} kpd \cdot (gf+gg)^2 \cdot \Big[(G1+gd)\cdot(G2+gg) + gf\cdot(G1+gd+G2+gg+gm)\Big] \\ +kpg \cdot gf \cdot \Big[(gf+gg)\cdot(G1+gd+gf)\cdot(1\cdot G2+gg+gf) - gf\cdot(gf-gm)\cdot(G2+gg+gf)\Big] \end{array} \right\} \\ +\sigma^2 Vg \cdot kpg \cdot G2^2 \cdot (gf-gm)\cdot(G2+gg+gf) \\ +Sdg \cdot kpg \cdot 2 \cdot G2 \cdot (G2+gg+gf)\cdot\Big[(gf+gg)\cdot(G1+gd+gf) - gf\cdot(gf-gm)\Big] \\ +Spd \cdot (gf+gg)^2 \cdot \Big[(G1+gd)\cdot(G2+gg) + gf\cdot(G1+gd+G2+gg+gm)\Big] \end{array}}{kpg\cdot(gf-gm)\cdot(G2+gg+gf)} \tag{17}$$

$$\sigma^2 p = \sigma^2 p_u + \frac{\begin{array}{c} (\sigma^2 eg \cdot G2^2 + \sigma^2 ig - \sigma^2 ig_c \cdot k \cdot 2 \cdot G2)\cdot\Big[kpd\cdot(gf-gm) + kpg\cdot(G1+gd+gf)\Big]^2 \\ +\sigma^2 id \cdot \Big[kpd\cdot(G2+gg+gf) + kpg\cdot gf\Big]^2 \end{array}}{\Big[(G1+gd)\cdot(G2+gg) + gf\cdot(G1+gd+G2+gg+gm)\Big]^2} \tag{18}$$

$$\sigma^2 p_g = \frac{(\sigma^2 eg \cdot G2^2 + \sigma^2 ig - \sigma^2 ig_c \cdot k \cdot 2 \cdot G2)\cdot\Big[kpd\cdot(gf-gm) + kpg\cdot(G1+gd+gf)\Big]^2}{\Big[(G1+gd)\cdot(G2+gg) + gf\cdot(G1+gd+G2+gg+gm)\Big]^2} \tag{20}$$

$$\sigma^2 p_d = \frac{\sigma^2 id \cdot \Big[kpd\cdot(G2+gg+gf) + kpg\cdot gf\Big]^2}{\Big[(G1+gd)\cdot(G2+gg) + gf\cdot(G1+gd+G2+gg+gm)\Big]^2} \tag{21}$$

TABLE XIII
CALCULATED PARAMETERS OF THE GAAS MESFET EQUIVALENT NOISE SOURCES SHOWN IN FIG. 1, FOR MEASUREMENT #3. R IS THE CROSS–CORRELATION COEFFICIENT BETWEEN eg AND ig. p_u IS THE PM NOISE THE MESFET GENERATES, WHICH IS NOT CORRELATED WITH THE EQUIVALENT LF FLICKER NOISE SOURCES

	Frequency range, Hz		
Parameter	40-400	200-2k	Units
$\sigma^2 eg$	$(3.8)^2$	$(2.7)^2$	$(\mu V/\sqrt{Hz})^2$
$\sigma^2 ig$	$(440)^2$	$(280)^2$	$(pA/\sqrt{Hz})^2$
$\sigma^2 id$	$(24)^2$	$(13)^2$	$(nA/\sqrt{Hz})^2$
$\sigma^2 p_u$	-137	-140	dBc/Hz
R	-79	-79	%

TABLE XIV
CONTRIBUTIONS OF THE GaAs MESFET NOISE SOURCES TO THE OVERALL PM NOISE $\sigma^2 p$ FOR MEASUREMENT #3

	Frequency range, Hz		
Parameter	40-400	200-2k	Units
$\sigma^2 p_u/\sigma^2 p$	2.9	2.4	%
$\sigma^2 p_g/\sigma^2 p$	97.0	97.5	%
$\sigma^2 p_d/\sigma^2 p$	0.1	0.1	%

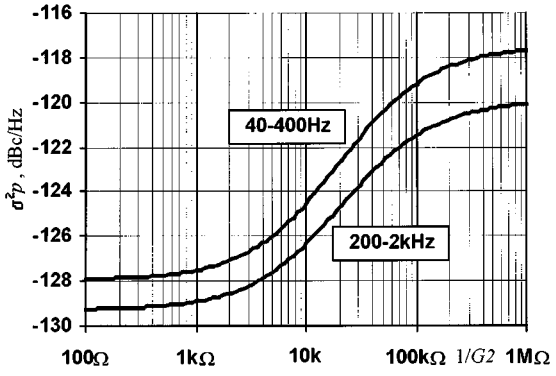

Fig. 9. Estimated level of the PM noise imposed on a 639-MHz RF carrier, when this is amplified by an AT-12 535 GaAs MESFET operating under the conditions in measurement #3, over a range of gate LF terminating conductances $G2$.

TABLE XV
COMPARISON OF PREDICTED AND MEASURED PM NOISE VALUES FOR MEASUREMENT #1

	Frequency range, Hz		
	40-400	200-2k	Units
Predicted PM noise $\sigma^2 p$, from equation (18)	-128	-129	dBc/Hz
Measured PM noise $\sigma^2 p_{MS}$, measurement #1	-130	-131	dBc/Hz

Equation (18) also makes it possible to observe the effects of LF terminating resistances on the PM noise generated by the GaAs MESFET. The dependence of the PM noise on the LF gate terminating resistance $1/G2$ thus calculated is shown in Fig. 9.

In measurement #1, the same GaAs MESFET was used as in measurement #3, again in 4-dB gain compression, but with $RG = 1$ kΩ instead of 39 kΩ; $1/G2$ for measurement #1 was 980 Ω. Table XV shows the PM noise level predicted for $1/G2 = 980\ \Omega$, using (18) and (19) with values (other than $G2$) from Tables VIII, XII, and XIII. The actual PM noise level measured in measurement #1 is also shown; a fair agreement is observed between the predicted and measured PM noise levels.

VIII. CONCLUSION

A noise measuring system has been developed that allows the simultaneous sampling of the LF noise on the gate and drain terminals of a GaAs MESFET, and the noise modulated onto an RF carrier when this is amplified by the MESFET. The LF noise on the gate of the GaAs MESFET has been found to be detectable using simple means, though the measuring system described requires further optimization for this measurement.

Preliminary results obtained using this measuring system have clearly demonstrated the validity of the flicker noise modulation theory for the excessive noise of GaAs MESFET oscillators. When the GaAs MESFET's tested were driven into 4-dB gain compression, a value commonly used in oscillators, it was found that, in most cases, the cross correlation between the LF noise on the drain of the MESFET's and the AM and PM noise sidebands on the amplified RF carrier approached 100%. Oscillators built around these devices, with the devices operating under the conditions shown, would exhibit high-level noise sidebands close to the carrier, which would be caused primarily by modulation of LF noise, as predicted by the theory.

The main objective of our study has been to develop a method for quantifying the levels and the cross-correlation coefficient of the effective internal GaAs MESFET flicker noise sources themselves (shown in Fig. 1), and the effect they have on the amplified RF carrier. The measuring system described can provide the information required for the calculation of many of these parameters, which can be extrapolated from the measurements taken.

A useful extension to this study would be the application of this procedure to a larger number of MESFET's, both of the same type (to observe parameter spreads), and of types with different physical construction and characteristics.

The results obtained from such an analysis could then be compared with the theory of generation and modulation of GaAs MESFET flicker noise, making it possible to obtain a better understanding of these mechanisms. The results should also assist in determining the optimal GaAs MESFET physical characteristics and operating conditions for minimum flicker and oscillator close-to-carrier sideband noise, enabling the design of GaAs MESFET oscillators with a better phase noise performance, and the development and optimization of GaAs MESFET oscillator noise-reduction techniques.

REFERENCES

[1] H. J. Siweris and B. Schiek, "Analysis of noise upconversion in microwave FET oscillators," *IEEE Trans. Microwave Theory*, vol. MTT–33, pp. 233–242, Mar. 1985.
[2] J. F. Sautereau *et al.*, "Large signal design and realization of a low noise X-band FET oscillator," in *Proc. 11th European Microwave Conf.*, Sept. 1981, pp. 464–468.
[3] B. T. Debney and J. S. Joshi, "A theory of noise in GaAs FET microwave oscillators and its experimental verification," *IEEE Trans. Electron Devices*, vol. ED-30, pp. 769–776, July 1983.
[4] H. Rohdin, C. Y. Su, and C. Stolte, "A study of the relation between device low frequency noise and oscillator phase noise for GaAs MESFETs," in *IEEE MTT-S Int. Microwave Symp. Dig.*, 1984, pp. 267–269.
[5] M. Camiade *et al.*, "Low noise design of dielectric resonator FET oscillators," in *Proc. 13th European Microwave Conf.*, 1983, pp. 297–302.
[6] P. H. Handel, "Nature of $1/f$ phase noise," *Phys. Rev. Lett.*, vol. 34, pp. 1495–1498, June 1975.

[7] C. P. Lusher and W. N. Hardy, "Effects of gain compression, bias conditions, and temperature on the flicker phase noise of an 8.5-GHz GaAs MESFET amplifier," *IEEE Trans. Microwave Theory Tech.*, vol. 37, pp. 643–646, Mar. 1989.
[8] B. Hughes *et al.*, "GaAs FET's with a flicker noise corner below 1 MHz," *IEEE Trans. Electron Devices*, vol. ED-34, pp. 733–741, Apr. 1987.
[9] P. A. Folkes, "Fluctuating deep level trap occupancy model for bulk 1/f noise in field-effect transistors," *Appl. Phys. Lett.*, vol. 55, pp. 2217–2219, Nov. 1999.
[10] C. Y. Su, H. Rohdin, and C. Stolte, "1/f noise in GaAs MESFETs," in *IEEE Int. Electron Device Meeting Dig.*, 1983, pp. 601–604.
[11] D. J. Day *et al.*, "Instability and gate voltage noise in GaAs metal–semiconductor field-effect transistors," *Can. J. Phys.*, vol. 67, no. 238, pp. 238–241, 1989.
[12] M. D. Das and P. K. Ghosh, "Gate current dependence of low frequency noise in GaAs MESFETs," *IEEE Electron Device Lett.*, vol. EDL-2, pp. 210–213, Aug. 1981.
[13] P. A. Folkes, "Characteristics and mechanism of 1/f noise in GaAs Schottky barrier field-effect transistors," *Appl. Phys. Lett.*, vol. 48, pp. 344–346, Feb. 1986.
[14] A. Van der Ziel *et al.*, "A theory of the Hooge parameters of solid state devices," *IEEE Trans. Electron Devices*, vol. ED-32, pp. 667–671, Mar. 1985.
[15] P. H. Handel, "Quantum approach to 1/f noise," *Phys. Rev. A, Gen. Phys.*, vol. 22, no. 2, pp. 745–757, Aug. 1980.
[16] J. Graffeuil *et al.*, "Low frequency noise physical analysis for the improvement of the spectral purity of GaAs FET oscillators," *Solid State Electron.*, vol. 25, pp. 367–374, 1982.
[17] S. Hashiguchi, N. Aoki, and H. Ohkubo, "Distribution of 1/f noise in an epitaxial GaAs MESFET," *Solid State Electron.*, vol. 29, pp. 745–749, 1986.
[18] M. Prigent and J. Obregon, "Phase noise reduction in FET oscillators by low frequency loading and feedback circuitry optimization," *IEEE Trans. Microwave Theory Tech.*, vol. MTT-35, pp. 349–352, Mar. 1987.
[19] A. N. Riddle and R. J. Trew, "A novel GaAs FET oscillator with low noise," in *IEEE MTT-S Int. Microwave Symp. Dig.*, 1985, pp. 257–260.
[20] J. Verdier, O. Llopis, R. J. Plana, and J. Graffeuil, "Analysis of noise up-conversion in microwave field-effect transistor oscillators," *IEEE Trans. Microwave Theory Tech.*, vol. 44, pp. 1478–1483, Aug. 1996.
[21] R. D. Martinez, D. E. Oates, and R. C. Compton, "Measurement and model for correlating phase and baseband 1/f noise in an FET," *IEEE Trans. Microwave Theory Tech.*, vol. 42, pp. 2051–2055, Nov. 1994.
[22] A. N. Riddle and R. J. Trew, "A new measurement system for oscillator noise characterization," in *IEEE MTT-S Int. Microwave Symp. Dig.*, 1987, pp. 509–512.
[23] K. H. Sann, "The measurement of near-carrier noise in microwave amplifiers," *IEEE Trans. Microwave Theory Tech.*, vol. MTT-16, pp. 761–766, Sept. 1968.
[24] P. A. Dallas and J. K. A. Everard, "Measurement of the cross correlation between baseband and transposed flicker noises in a GaAs MESFET," in *IEEE MTT-S Int. Microwave Symp. Dig.*, 1990, pp. 1261–1264.
[25] S. C. F. Lam *et al.*, "Analytical model of GaAs MESFET output conductance," in *IEEE Int. Electron Device Meeting Tech. Dig.*, 1988, pp. 203–206.
[26] F. G. Stremler, *Introduction to Communication Systems, 2nd ed.*. Reading, MA: Addison-Wesley, 1982.
[27] E. O. Brigham, *The Fast Fourier Transform*. Englewood Cliffs, NJ: Prentice-Hall, 1974.

Paul A. Dallas (S'88–A'95) received the B.Sc. and Ph.D. degrees from King's College, University of London, London, U.K., in 1987 and 1995, respectively.

From 1997 to 1999, he was with the Satellite Communications Department, Racal Avionics Ltd., London, U.K., where he is involved in the design and development of airborne satellite communications equipment. He is currently with the Hellenic Aerospace Industry SA, Tanagra, Greece.

Jeremy K. A. Everard (M'90) received the B.Sc. Eng. degree from King's College, University of London, London, U.K., in 1976, and the Ph.D. degree from the University of Cambridge, Cambridge, U.K., in 1983.

Over a period of six years, he was with the GEC Marconi Research Laboratories, M/A-Com, and Philips Research Laboratories where he worked on radio and microwave circuit design. While with Philips, he ran the Radio Transmitter Project Group. He then taught RF and microwave circuit design, opto-electronics and electromagnetism at King's College London, for nine years while leading the Physical Electronics Research Group. In 1990, he became a University of London Reader in Electronics at King's College London and Professor of electronics at the University of York, in September 1993. His current research interests in opto-electronics include all optical self-routing switches that route data-modulated laser beams according to the destination address encoded within the data signal, ultrafast three-wave opto-electronic detectors, mixers, and phase-locked loops, and distributed fiber optic sensors. In the RF/microwave area, his interests include the theory and design of low-noise oscillators using inductor capacitor (*LC*), surface acoustic wave (SAW), crystal, dielectric, transmission line, helical, and superconducting resonators, flicker noise measurement and reduction in amplifiers and oscillators, high-efficiency broad-band amplifiers, high Q printed filters with low radiation loss and monolithic-microwave integrated-circuit (MMIC) implementations. He has published over 50 papers, co-edited and co-authored a book on gallium arsenide technology and its impact on circuits and systems and contributed to a book on optical fiber sensors. He has filed for 15 patents.

Dr. Everard is a member of the Institution of Electrical Engineers (IEE), London, U.K.